Focusing on Information Context for ITS using a Spatial Age of Information Model

Julian Heinovski*, Jorge Torres Gómez, Falko Dressler

School of Electrical Engineering and Computer Science, TU Berlin, Germany

Abstract

New technologies for sensing and communication act as enablers for cooperative driving applications. Sensors are able to detect objects in the surrounding environment and information such as their current location is exchanged among vehicles. In order to cope with the vehicles' mobility, such information is required to be as fresh as possible for proper operation of cooperative driving applications. The age of information (AoI) has been proposed as a metric for evaluating freshness of information; recently also within the context of intelligent transportation systems (ITS). We investigate mechanisms to reduce the AoI of data transported in form of beacon messages while controlling their emission rate. We aim to balance packet collision probability and beacon frequency using the average peak age of information (PAoI) as a metric. This metric, however, only accounts for the generation time of the data but not for application-specific aspects, such as the location of the transmitting vehicle. We thus propose a new way of interpreting the AoI by considering information context, thereby incorporating vehicles' locations. As an example, we characterize such importance using the orientation and the distance of the involved vehicles. In particular, we introduce a weighting coefficient used in combination with the PAoI to evaluate the information freshness, thus emphasizing on information from more important neighbors. We further design the beaconing approach in a way to meet a given AoI requirement, thus, saving resources on the wireless channel while keeping the AoI minimal. We illustrate the effectiveness of our approach in Manhattan-like urban scenarios, reaching pre-specified targets for the AoI of beacon messages.

Key words: Age of information; vehicular networking; cooperative driving; intelligent transportation systems; beaconing

1. Introduction

Vehicles are becoming more capable in terms of sensors and computing power, we can already see first deployments of intelligent transportation systems (ITS). They are able to do real-time monitoring of their surrounding environment, which allows detection of objects such as other vehicles or pedestrians. Such a detection can help in taking driving decisions and might be performed collaboratively among vehicles. Vehicle-to-everything (V2X) communication technologies such as IEEE 802.11p (often referred to as distributed short-range communication (DSRC)), and cellular V2X (C-V2X) allow exchanging of information with other vehicles or roadside infrastructure. Such communication capability enables cooperative driving applications, which bring a set of new features and services for today's driving, but also demands new communication strategies for proper operation [1].

Such applications require fresh (up-do-date) information from other vehicles to operate properly. Due to the inherent mobility of ITS, location-information may become outdated and eventually no longer relevant to an application because of position changes. To ensure up-to-date information, vehicles exchange their location with regular *beacons* messages, such as cooperative awareness messages (CAMs) [2]. Freshness of such information does not only depend on frequent beacons' transmissions but also on the network capacities, which can lead to packet collisions and the loss of data.

Balancing requirements to update beacons regularly and network capacities, the concept of the age of information (AoI) provides a framework to evaluate information freshness [3, 4]. The AoI metric complements raw delay, loss, and throughput in the network, which in turn accounts for the process of emission and delays introduced in the communication chain, all-together [3]. Inherently, this distinguishes AoI metrics from conventional delay metrics [5], allowing to optimize of the network freshness as the best balance between throughput and delay.

Recent research illustrates the use of AoI metrics in the vehicular context. The average AoI and the peak age of information (PAoI) are used to find the best strategy for the emission rate of beacon packets, see for instance [6, 7, 8, 9, 10, 11, 12] (further discussion in the next Section). However, these metrics do not consider information context [13]; not all packets necessarily carry the same information's importance, thereby not introducing the same level of freshness for the status update. To illustrate the significance of information context, let us consider an in-

*Corresponding author

Email addresses: heinovski@ccs-labs.org (Julian Heinovski), torres-gomez@ccs-labs.org (Jorge Torres Gómez), dressler@ccs-labs.org (Falko Dressler)

Article published in Elsevier Computer Communications 209 (2023) 203–216. (10.1016/j.comcom.2023.07.002)

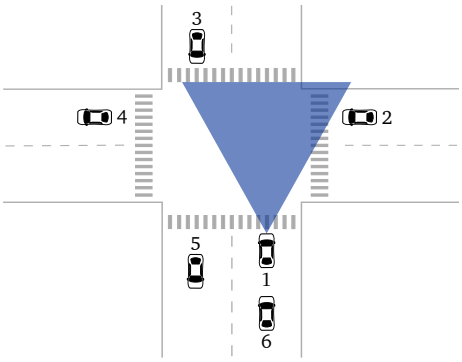

Figure 1: Example scenario: Vehicles in the direction of movement of vehicle 1 (vehicles 2 and 3) are more relevant than others (vehicles 4, 5, and 6) when considering a safety application such as ICA.

tersection collision avoidance (ICA) scenario as depicted in Fig. 1. Focusing on vehicle 1, the status updates of the vehicles in front (i.e., vehicles 2 and 3) are more critical to avoid potential collisions than those from the other vehicles (i.e., vehicles 4, 5, and 6). Thus, it is preferable to collect updated information about vehicles 2 and 3 rather than 4, 5, and 6 in order for vehicle 1 to avoid collisions at this intersection. In this sense, we intent for an AoI-based metric to account for this application-dependent information context.

In the literature, some reported studies address the information's content with the AoI. Examples include techniques to best predict *Markovian* sources [14], to better synchronize cache content with the remote source [15], to account for only newly arrived information [5, 16], and to use information-theoretic approaches for reduced uncertainty about the source [3].

In a different approach, we consider the transmitting vehicle's location as a metric to quantify the importance of their information. We emphasize such importance with weighting coefficients to evaluate the average PAoI metric in the context of cooperative driving. These coefficients inherently devise some filtering of received packets, which allows for treating vehicles' information more selectively. Using our model allows focusing on timely updates of relevant vehicles only for meeting a given AoI requirement.

In this paper, which is an extension of the previous work in [17], we further report on the impact of the scenario on the PAoI when applying our spatial model. In addition, we demonstrate the practical use of the proposed model by applying it to an AoI-based beacon adaption algorithm.

Our main contributions can be summarized as follows:

- We propose a spatial model for interpreting the AoI of received packets based on the spatial location of the transmitting vehicle, making AoI context specific.
- We evaluate the AoI and the impact of our model on individual communication links and the overall network.
- We show that using our model helps controlling the beacon rate necessary for achieving a given AoI requirement.
- We demonstrate the practical use of the proposed model by applying it to an AoI-based beacon adaption algorithm.

Elaborating on the above contribution, the paper is structured as follows. We discuss in further detail the use of AoI metrics in the vehicular context in Section 2. We present the new AoI model and introduce the weighting coefficient in Section 3 with the corresponding analytic description. We also introduce in Section 4 an adaptive mechanism for the beacon rate with the proposed AoI model using a proportional-integral-derivative (PID) controller. In Section 5, we assess the performance of the proposed model and the adaptive algorithm to meet freshness requirements. Finally, we sketch some concluding remarks in Section 7.

2. Age of Information in ITS

Following the standard IEEE 802.11p, we already see a number of studies that address the use of AoI metrics for time-critical applications in vehicular networks [6, 7, 8, 9, 10, 11, 12] and including test-bed demonstrators [18]. The AoI metric is reported to update the network freshness for the exchange of vehicles' speeds and positions. Some of these works provide closed-form expressions for the AoI metric [8, 9, 10, 11], while other works estimate the average AoI metric numerically [6, 7].

Accounting for the AoI metrics, other works use analytic methods for the average AoI [9] and PAoI [12]. The average AoI metric is formulated mainly in two different approaches. On one hand, Lyamin et al. [9], Vinel et al. [19] straightly formulate the average AoI as the average of the time duration between two consecutive received packets. They assume that the time duration distributes according to the joint event where two transmissions do not collide in the channel. The channel collision probability is evaluated according to the formulation provided by Vinel et al. [19].

On the other hand, the average AoI is evaluated using the formula for the remaining service time in a queue [8, 11] and considering the hidden [8, 11] and non-hidden node problem scenario [10]. In the hidden node scenario, the time duration of message transmissions is expanded, assuming that hidden nodes transmit independently with a random phase between 0 and the transmission duration parameter. In the non-hidden scenario, Andrea et al. [10] also derive a formula for node and network levels. The node-level accounts for the average AoI at any arbitrary node, assuming they only transmit the most recent packet. The network level evaluates the case where nodes do not transmit new packets till the current one is sent. In this case the network is modeled according to a Markov chain model, the transition probabilities can be derived [19].

In a different direction, based on simulation results, the existence of a unique beacon period minimizing the

average AoI is illustrated for a certain number of vehicles, and contention window (CW) sizes [6]. Following these results, a rate control algorithm is derived from adapting the broadcast period based on local measurements of the average AoI. The vehicle reduces or increases the beacon period by comparing it to the estimated average AoI metric looking for the maximum network freshness.

All the above studies conduct simulations based on the IEEE 802.11p standard for single-hop [6, 8, 11, 9, 8] and multi-hop [7, 8, 6, 7] networks. Besides, a variety of scenarios for the traffic of vehicles have been studied. Examples include four lane roads [6], highways [12, 18], platooning [7, 9], the more artificially Manhattan Grid [8, 11, 18], the TapasCologne scenario [8, 11], and open environments [10]. Furthermore, the work in [18] recreates a traffic scenario integrating simulators with software defined radio (SDR) devices.

However, these reported solutions are only addressing protocol parameters (e.g., beacon rate, CW size) and the channel impact (e.g., collisions, noise) to formulate the average AoI metric. Addressing information context, Michalopoulou et al. [20] seek to minimize the information aging in the spatial dimension when evaluating the product of the speed of the vehicle and the time duration between received packets. The information age is reduced by stating the optimization problem in the spatial domain to minimize the predicted location error. Also in the spatial domain, Parella et al. [21] implement a penalty function for the AoI, addressing a better prediction trajectory of neighboring vehicles. The penalty function (dependent on the AoI of CAM messages) is defined using the distance difference between the true and predicted position of the neighboring vehicles. The importance of information can also be considered as a weight factor on the average AoI metric. Zhang et al. [22] evaluate the weight while balancing the message's priority, persistence, and reliability.

In a different approach, we introduce a degree of importance in the AoI metrics concerning the intended direction of the vehicle and its surrounding. In the form of weighting coefficients as formulated by Sorkhoh et al. [23], we incorporate into the average PAoI metric the vehicular context (direction, surrounding), looking for some meaning of received beacon packets [4]. In doing so, we study the PAoI metric weighting as more critical for those vehicles in the direction of movement (cf. Fig. 1) and with less importance otherwise, when considering a safety application such as ICA [24] as an example use case. We use this modified PAoI metric and compare it to a similarly modified AoI requirement of 100 ms, which is often used in literature as desired update interval [25, 26]. We thus identify how many vehicles have fresh information, similar to using the original AoI definition.

3. A Spatial Model for the AoI

Typically, the AoI metrics are measured per user irrespective of their location. All the packets received from surrounding vehicles are treated with equal importance. However, the level of importance is application dependent: E.g., while in platooning only the members of the platoon itself are relevant, it is the surrounding vehicles within the direction of movement that are important for safety-related applications such as ICA. As one example use case, Fig. 1 thus shows such an intersection scenario. Here, the most valuable information for vehicle 1 will be located in the direction of its movement (shadowed area). Thus, vehicles within this area (i.e., vehicles 2 and 3) should be assigned a higher level of importance than other vehicles in the surrounding. Beacon packets coming from vehicles in the rear of the intended direction will not be that informative about the traffic in the intended direction of vehicle 1. Therefore, vehicles in front will be more demanded to reduce the corresponding AoI metrics than the vehicles in the rear. Since all vehicles are equal in the standard AoI, frequent beacon transmissions from the less important vehicles can lead to unnecessary channel load in this case. If the communication protocol was aware of this application-specific level of importance, it could update the periodicity of the beacons in accordance and eventually reduce the load on the wireless channel.

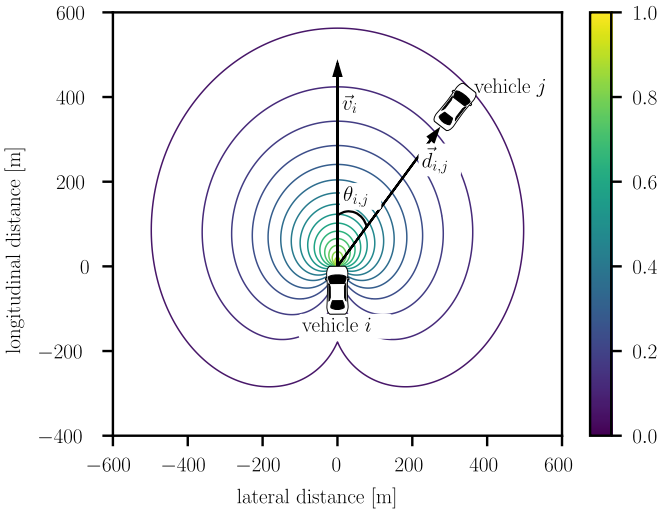

Figure 2: Visual representation of our spatial model for calculating the weighting coefficient used for the AoI interpretation with an example configuration of $\alpha = 0.75, \beta = 0.005$.

3.1. Weighted Peak AoI

To consider the location of the transmitting vehicle as a metric of importance to the information, we propose a new way of interpreting the AoI. To that end, we introduce a weighting coefficient that is applied to the PAoI metric as well as to an AoI requirement, emphasizing on packets from important vehicles. Thereby, we introduce some level of selectivity for the received packets which allows to treat vehicles' information differently according to the importance to the application. Our model can be easily adjusted to the requirement of a specific application through parameters and does not modify the underlying AoI metric itself.

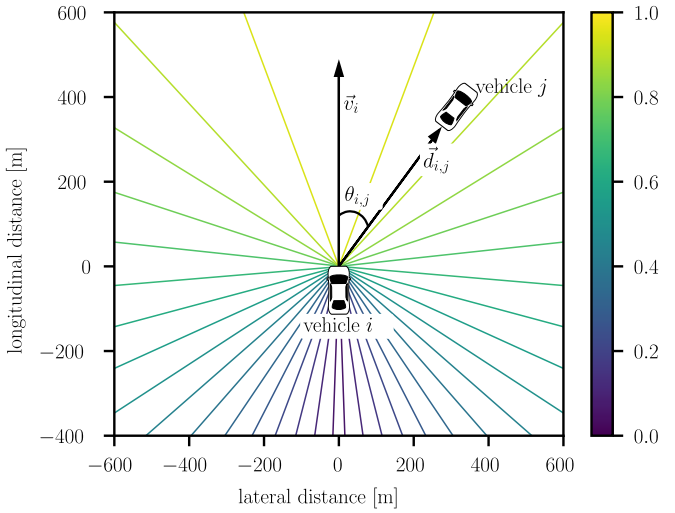

Figure 3: Visual representation of our spatial model for calculating the weighting coefficient used for the AoI interpretation with an example configuration of $\alpha = 0.5, \beta = 0$. This configuration only takes the angle between vehicles i and j into account.

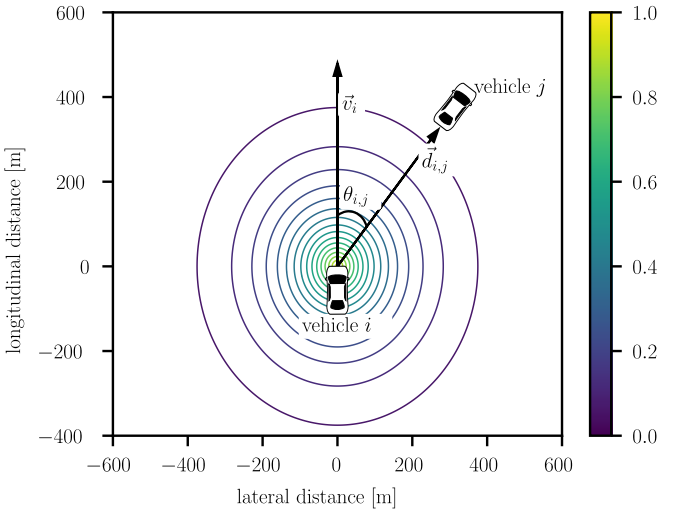

Figure 4: Visual representation of our spatial model for calculating the weighting coefficient used for the AoI interpretation with an example configuration of $\alpha = 0, \beta = 0.0075$. This configuration only takes the distance between vehicles i and j into account.

We choose the weighting coefficient as a raised-cosine function with a decay factor as

$$\omega_{j,i} = \frac{1}{2}\left(1 + \cos(\alpha\theta_{i,j})\right) e^{-\beta\|\vec{d}_{i,j}\|} \quad , \tag{1}$$

where $\theta_{i,j}$ is the angle between the transmitting vehicle j and the direction of movement of vehicle i and $\| \vec{d}_{i,j} \|$ is the distance between both vehicles, while α and β are two coefficients to select the degree of selectivity in the spatial domain. The coefficient α provides selectivity in the radial direction, while β in the azimuth direction. The larger the value of α or β is, the narrower is the beam of vehicle i. Fig. 2 shows a visual representation of our weighting coefficient with an example configuration of $\alpha = 0.75, \beta = 0.005$.

To derive the angle and the distance between vehicles, we assume that vehicles are equipped with global positioning system (GPS) receivers, and that this information is exchanged between vehicles in periodic beaconing messages. Using the configuration in Fig. 2, $\omega_{j,i}$ is close to 1 whenever vehicle j is in the direction of movement of vehicle i. Otherwise, it is close to 0 whenever vehicle j is away, being 0 when vehicle j is located at the rear of vehicle i.

In order to parameterize our proposed model, one needs to select values for the model parameters α and β. Since these will determine the relevance of vehicles' information, their values have to be selected carefully and application-dependent. In order to give further intuition on the behavior of these, Figures 3 and 4 show visual representations of two more example configurations. In Fig. 3, the distance between vehicles is not used for calculating the weighting coefficient $\omega_{j,i}$ due to a value of 0 for β. Thus, the area around the vehicle i is mapped to the coefficient $\omega_{j,i}$ by the cosine-part of Eq. (1), using the angle towards vehicle j. Here, a close vehicle and a far-away vehicle will receive the same value for $\omega_{j,i}$ if their angle towards vehicle i is the same. In contrast, in Fig. 4, the angle between vehicles is not used for calculating the weighting coefficient due to a value of 0 for α. Thus, the distance from vehicle i to other vehicles is mapped to the coefficient $\omega_{j,i}$ by part with Euler's number of Eq. (1).

With this coefficient, we measure the importance of the introduced age per received packet using the average PAoI metric as

$$\Delta_{j,i}^{(\omega)} = \omega_{j,i}\Delta_{j,i}^{(p)} \quad , \tag{2}$$

where $\Delta_{j,i}^{(p)}$ denotes the average PAoI metric for a link between vehicles j and i. Correspondingly, the combined PAoI per neighboring vehicle j at vehicle i will be calculated after averaging the perceived $\Delta_{j,i}^{(p)}$ as

$$\Delta_{i}^{(\omega)} = \frac{1}{N-1}\sum_{j=1}^{N-1} \omega_{j,i}\Delta_{j,i}^{(p)} \quad . \tag{3}$$

Finally, we account for the network operation after averaging for the total of nodes as

$$\Delta^{(\omega)} = \frac{1}{N(N-1)}\sum_{i=1}^{N}\sum_{j=1}^{N-1} \omega_{j,i}\Delta_{j,i}^{(p)} \quad . \tag{4}$$

The average PAoI ($\Delta_{j,i}^{(p)}$) can be derived by analytical or numerical means through simulators. Analytically, it can be obtained after calculating the expected average of the inter-arrival (Y_n) and system time (T_n) as $\Delta_{j,i}^{(p)} = \mathbb{E}\{Y\} + \mathbb{E}\{T\}$ when all packets emitted are received [13]. However, some packets will not be successfully received due to the system and channel conditions (e.g., collisions, replacement of the old beacon frames, low reliability during their reception, etc.) [19]. Taking into account the impact of the system

and channel effects in the packet reception process, as given by the successful probability P_{sd}, the average PAoI can be calculated as

$$\Delta_{j,i}^{(p)} = \frac{1}{P_{sd}}\mathbb{E}\{Y\} + \mathbb{E}\{T\} \quad , \tag{5}$$

where the value for P_{sd} in Eq. (5) can be directly computed considering the impact of noise and collisions using the closed-form expressions in [19, Eq. (7)], or through simulations.

The Eq. (5) can be directly computed by recalling the use of the negative binomial distribution as described in [27]. However, it can be intuitively derived based on the meaning of the related variables in Eq. (5). P_{sd} can be interpreted as the ratio of successfully transmitted packets; thus, its inverse will provide the total of attempts to have a successful transmission. Therefore, the first term in Eq. (5) will provide the waiting period before a packet is successfully transmitted. Adding the average time spent on the system ($\mathbb{E}\{T\}$) will thus provide the average PAoI.

3.2. Remarks

The introduced coefficients in Eq. (3) provide a mean to "filter" packets according to their relevance. For instance, in the intersection scenario depicted in Fig. 1, the average PAoI of packets from the vehicles 4, 5, and 6 will be lowered as less relevant, thus emphasizing those packets from vehicles at the front side of vehicle 1 (vehicles 2 and 3). In this way, the resulting average PAoI will be characterized the most by those links of interest according to the application context.

Eq. (3) is also useful in different ITS scenarios, and, also with a different dependency for the coefficients other than Eq. (1). Overall, the Eq. (3) comprises a mean to emphasize some communication links in contrast to others. Once the links of interest are determined, they will shape the resulting average PAoI whenever their corresponding coefficients are close to 1. In contrast, those links whose coefficients are close to 0 will not contribute to the age of information metric.

Besides, we selected the dependency of the coefficients with the spatial coordinates in Eq. (1) as a two-dimensional function in two separable terms. One dimension for the azimuth direction defines the raised-cosine function [28], which conveniently allows multiplying by 0 to those packets coming from the rear side of vehicle i. The second dimension is in the radial direction and defines a decay factor, which decrements as long as the distance increases. Overall, both terms let to a function that is also all-orders differentiable, which accounts for its mathematical tractability.

3.3. Weighted Target AoI

The derived weighted PAoI metric can be used to fairly evaluate the freshness of the status updates with a given target, i.e., when the age of received packets is less than a given threshold. This approach is particularly relevant when we want to save resources looking at the PAoI metric just performing below a given threshold T (target). In this way, we avoid the network to operate on the minimum average where demanding resources are higher. After applying the same weighting coefficient (cf. Eq. (1)) to a given threshold T by

$$T_{j,i}^{(\omega)} = \omega_{j,i} T \quad , \tag{6}$$

we can compare the derived average PAoI with the weighted target $T_{j,i}^{(\omega)}$

$$\Delta_{j,i}^{(\omega)} \leq T_{j,i}^{(\omega)} \tag{7}$$

for a link between vehicles j and i. A single vehicle i can to this for all of its neighboring vehicles j by

$$T_{i}^{(\omega)} = \frac{1}{N-1}\sum_{j=1}^{N-1} \omega_{j,i} T_{j,i} \tag{8}$$

and

$$\Delta_{i}^{(\omega)} \leq T_{i}^{(\omega)} \quad . \tag{9}$$

Correspondingly, we account for the network operation after averaging for the total of nodes as

$$T^{(\omega)} = \frac{1}{N(N-1)}\sum_{i=1}^{N}\sum_{j=1}^{N-1} \omega_{j,i} T_{j,i} \tag{10}$$

and

$$\Delta^{(\omega)} \leq T^{(\omega)} \quad . \tag{11}$$

Further discussions on the utility of these expressions and their interpretation are given within Section 5.

4. Adaptive Beaconing based on AoI

In this section, we aim to show the practical use of our spatial model for cooperative driving by applying it to an algorithm for adapting the beacon rate based on the age of information. We use a simple proportional-integral-derivative (PID) controller-based algorithm that controls a vehicle's beacon rate based on PAoI measurements from neighboring vehicles. In contrast to other work from the literature [6, 29], our goal is to keep peak AoI values below a fixed requirement (100 ms), rather than achieving minimal AoI for all nodes. Applying our spatial model should help to focus on relevant vehicles while selecting the beacon rates.

4.1. Communication Setup

Fig. 5 shows the two-hop mechanism of our adaption approach which is used to evaluate the weighted PAoI $\Delta_{i}^{(p)}$ locally at vehicle i, according to Eq. (3). Since the information in the beacons of vehicle i are relevant to vehicles j and k, the AoI as well as the information's relevance (given by the weighting coefficient) needs to be computed at vehicles j and k. As only vehicle i can control

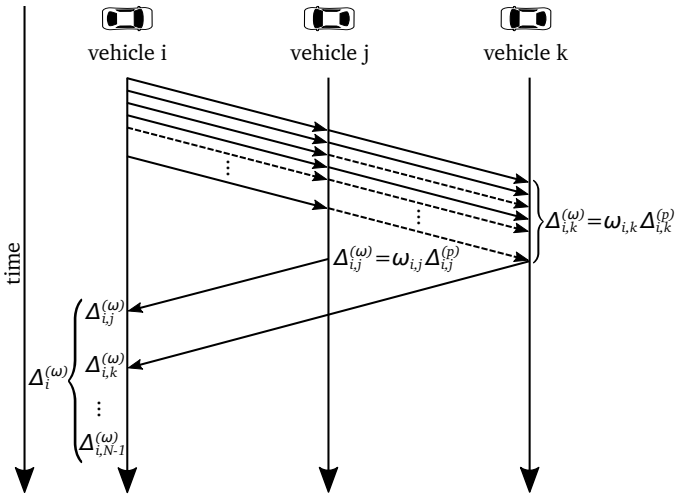

Figure 5: Two-hop mechanism of our adaption approach for evaluating the weighted PAoI at vehicle i.

its beacon rate, we need this two-hop mechanism to inform i about any required changes. Note that the indices i and j here are different in comparison to Section 3.

In the first hop, vehicles j and k compute the weighted PAoI $\Delta_{i,j}^{(\omega)}$ and $\Delta_{i,k}^{(\omega)}$ upon reception of a beacon from vehicle i. This is done based on Eq. (1) and the spatial locations of the corresponding vehicles. In the second hop, vehicle j and k transmit these weighted PAoI values to vehicle i within their own regular beacons. In this way, vehicle i is able to compute $\Delta_i^{(\omega)}$ by averaging all weighted PAoI measurements from its neighbors j and k, following Eq. (3). $\Delta_i^{(\omega)}$ here corresponds to the freshness of i's information as a combined perspective from vehicle j and k. Following the same procedure, vehicle i also computes the weighted target AoI T_i^{ω} using Eq. (8). Vehicle i is now able to evaluate the freshness of its own information $\Delta_i^{(\omega)}$ perceived at vehicles j and k against the shared requirement T_i^{ω}. Thus, it can determine whether the information is fresh enough and whether it needs to adjust its beacon rate.

4.2. Beacon Adaption Algorithm

We use a PID controller [30] on all vehicles to adjust their beacon rate such that PAoI values converge to the target AoI. To achieve this, we use the PAoI as input and the target AoI as set-point for the PID controller. A PID controller in general consists of (1) a **P**roportional part, which produces a control output proportional to the error between the set-point and the actual output, (2) an **I**ntegral part, which accumulates the error over time and generates an output proportional to the integrated error, and (3) a **D**erivative part, which produces an output proportional to the rate of change of the error. The controller output is given by

$$u(t) = G_P \cdot e(t) + G_I \cdot \int e(t)\ dt + G_D \cdot \frac{de(t)}{dt} \quad , \quad (12)$$

where $u(t)$ is the controller output at time t, $e(t)$ is the error (difference to the set-point) at time t, $\int e(t)\ dt$ is the integral of the error over time (the accumulated error), and $\frac{de(t)}{dt}$ is the derivative of the error with respect to time (the rate of change of the error). G_P, G_I, and G_D are gain coefficients to control the impact of the individual parts of the PID controller towards the output.

As input and set-point for the PID controller, we specifically use the average weighted PAoI measurement $\Delta_i^{(\omega)}$ and the average weighted target AoI $T_i^{(\omega)}$, respectively. Thereby, we expect the controller to eventually select beacon rates that result in the PAoI measurements converging to the target AoI. We implement the individual terms of Eq. (12) in the following way. The error $e(t)$ at vehicle i in iteration t is given by

$$e(t) = T_i^{(\omega)} - \Delta_i^{(\omega)} \quad (13)$$

and the derivate error $de(t)$ evaluated in the discrete domain as

$$\frac{de(t)}{dt} \approx \frac{e(t-\Delta t) - e(t)}{\Delta t} \quad , \quad (14)$$

using only the error from the previous algorithm execution. The gain coefficients for the individual parts of the PID controller are chosen by observing the stable system behavior. We use $G_p = 1.0$, $G_I = 0$, thereby disabling the integral part, and $G_D = 0.1$.

Using Eq. (12), the adjustment $u(t)$ of the current beacon interval λ_i at vehicle i in iteration t is calculated and added to the current beacon interval λ_i. We update the new beacon interval within the limits of 10 ms (100 Hz) and 100 s (0.01 Hz), such that only valid beacon rates are produced. The algorithm is executed on a regular basis (i.e., at an interval of 2 × target AoI) on all vehicles individually.

5. Evaluation

In this section, we evaluate the PAoI and the impact of the weighting coefficient $\omega_{j,i}$ from our spatial model (see Section 3). For this, we perform simulative experiments within the Veins simulator [31]. First, we provide an initial analytical assessment of our model in Section 5.1. After that, we consider simulative results and discuss the impact of the link distance on the standard PAoI in Section 5.3. We continue selecting two specific link distances (i.e., a short and a long one) and analyze the combined PAoI without and with our spatial model in Sections 5.4 and 5.5. Next, we show the impact of our spatial model on the network PAoI in Section 5.7. Afterwards, we analyze the impact of the model parameters and the scenario on the network PAoI in Sections 5.8 and 5.9. Finally, we analyze the behavior of our AoI-based algorithm for adapting the beacon rate from Section 4 in Section 5.10.

5.1. Initial Analytical Assessment

To provide further intuition on the impact of the coefficient $\omega_{j,i}$, we now perform an initial analytical assessment

Parameter	Value
Scenario Size	550 m × 550 m
Simultaneous Vehicles N	200
Beacon Size L	512 Byte
Bitrate R	6 Mbit/ sec
CW size W	4–8
Preamble duration T_{P}	32 µ sec
PLCP duration T_{PLCP}	8 µ sec
Propagation delay δ	1 µ sec
AIFS	58 µ sec

Table 1: Parameters used for analytical evaluation

Parameter	Value
Scenario Type	Manhattan Grid
Simulation Time	10 s
Beacon Rates	1, 2, 5, 8, 10, 16, 20, 25, 40, 50, 100 Hz
Carrier Frequency	5.89 GHz
Access Category	AC_VO
EDCA Queue Size	1
TX Power	20 mW
Attenuation Model	Free-space only ($\alpha = 2$)

Table 2: Additional parameters used for simulation experiments

of the perceived average PAoI given by Eq. (3). We compute it for a given link between 200 vehicles that are all moving randomly in a free-space grid. The corresponding communication parameters are listed in Table 1. To compute $\Delta_{j,i}^{(p)}$, we use Eq. (5) where the probability of successful beacon reception P_{sd} is obtained from simulation (cf. Sections 5.2 and 5.3). We consider a contention-based communication system according to IEEE 802.11p, where vehicles broadcast beacon messages following a collision avoidance mechanism without retransmissions. Frames are emitted after verifying free channel access during the arbitration inter-frame space (AIFS) and CW time windows. We assume that only the most updated message is queued at the emitter, waiting for a free slot to be transmitted [8].

Figures 6 and 7 plot analytical results for the impact of the model parameters α and β, which define the degree of selectivity for computing the PAoI metric. The case $\alpha = 0$, $\beta = 0$ results in $\omega_{j,i} = 1$, i.e., no spacial selectivity at all, which corresponds to highest PAoI metric (standard definition from Eq. (5)). However, as α and β increase, the perceived PAoI metrics are reduced due to the reduced importance of those vehicles not in the direction of movement and not that close to the moving vehicle (cf. link 1-5 in Fig. 1). In this case, the contribution of the given link to the total PAoI in Eq. (3) will become less, thus less critical. Comparing both figures indicates that the distance has a higher impact on the calculation of the weighting coefficient than the angle.

5.2. Simulation Setup

After the initial analytical assessment of our model, we now move on and consider simulative results. For our simulation, we use the well-known vehicular network simulation framework Veins [31] to enable a realistic evaluation. In

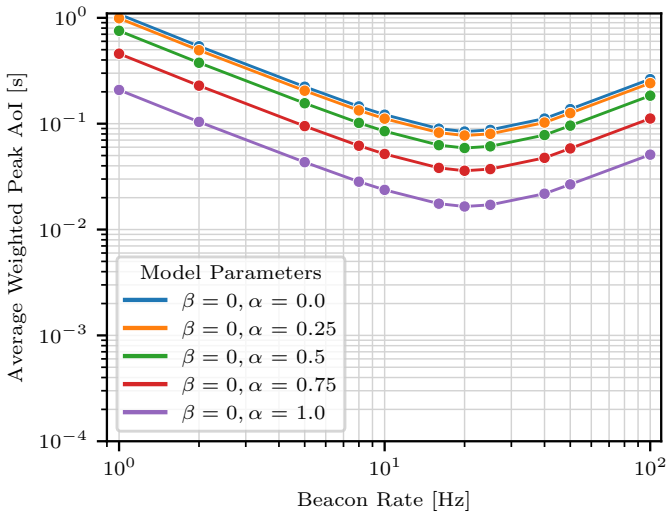

Figure 6: Average PAoI for different angle coefficients when $\beta = 0$. The spatial model only focuses on the angle.

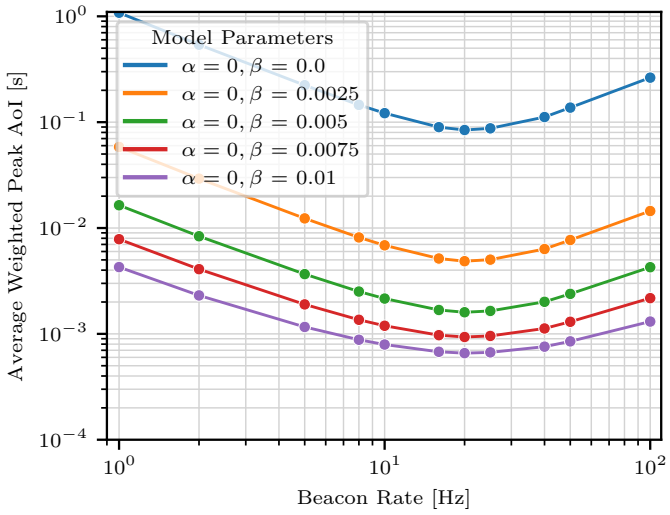

Figure 7: Average PAoI for different distance coefficients when $\alpha = 0$. The spatial model only focuses on the distance.

particular, we use OMNeT++ 5.6.2, SUMO 1.6, and Veins 5.1. Tables 1 and 2 together summarize the most important parameters used in our simulations.

We focus on an urban simulation environment and, for simplicity, chose a 550 m × 550 m Manhattan grid scenario (see Fig. 8). The scenario contains 200 vehicles that depart at random positions and follow random trips. Vehicles are transmitting beacons such as CAMs via IEEE 802.11p at a static beacon rate. In our simulation, we are able to switch off the attenuation effect of buildings by disabling the *obstacle shadowing* [32]. Furthermore, we modified the medium access control (MAC)-layer queue to replace the most recent packet if the maximum queue size is reached and a new beacon was generated from the application layer. Together with a queue size of 1, this results in always transmitting the most recent data in the beacon [8].

The data from the received packets including its gen-

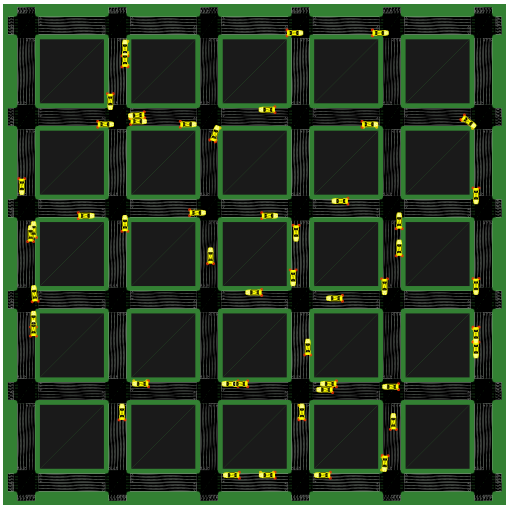

Figure 8: Manhattan grid with randomly distributed vehicles

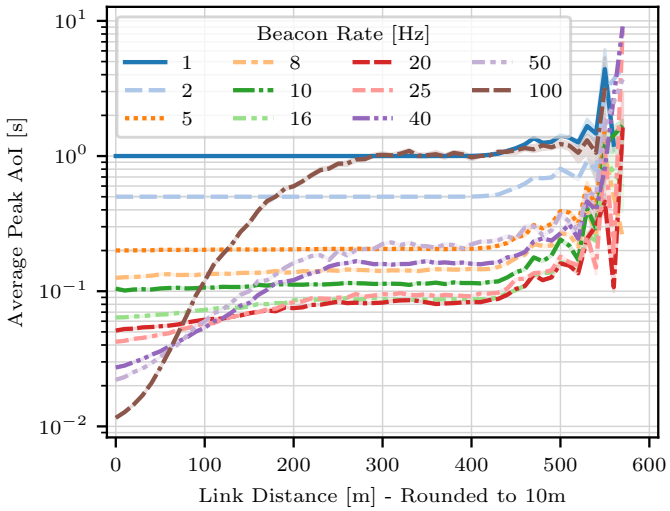

Figure 9: Average PAoI based on the link distance (rounded to 10 m) with different beacon rates

eration and reception times is stored in a simple 1-hop neighbor table on every vehicle. We are thus able to calculate the standard AoI for a given link by using this time stamp of the last successfully received update. Whenever a new beacon from vehicle j is received by vehicle i, the data as well as the time stamp is updated and we record the PAoI as the current AoI value of this link at i. Similarly, we calculate the weighting coefficient according to Eq. (1) for a particular link upon successful packet reception by using the sender's position from within the packet. Thus, these values are only calculated upon reception of at least the second beacon. From our simulation, we obtain, on average, a total of 1500 samples for PAoI and corresponding target AoI per vehicle and simulated beacon rate, which we are going to use for the following results.

5.3. Impact of Link Distance on Standard AoI

In order to underline the issues with the standard AoI, we first have a look at the impact of the link distance on the AoI. The PAoI, as defined in Eq. (5), is influenced by the beacon rate (cf. $\mathbb{E}\{Y\}$), system delay (cf. $\mathbb{E}\{T\}$), and probability of successful packet reception (cf. $\frac{1}{P_{sd}}$). Thus, even if multiple vehicles use the same beacon rate for beacon transmission, the observed PAoI metrics can be very different due to the effects of the wireless communication channel, especially over large distances. Since the longest possible distance between two vehicles in our scenario is only about 780 m, we can neglect the system delay as an influencing factor.

The probability for successful reception of a packet, however, has to be considered. It depends on the signal-to-noise-and-interference-ratio (SNIR), which is, among others, influenced by scenario-related effects such as attenuation of the signal as well as interference from other vehicles. In our scenario, the signal is attenuated by free-space path loss, which weakens its strength proportional to the link distance. Also, at large distances, hidden nodes can introduce additional interference and collisions, which further degrades the SNIR. At some point, a packet cannot be received successfully anymore and the AoI of the corresponding link increases further until the next successful reception. Therefore, the link distance can have a huge impact on the PAoI, especially for far away vehicles.

Fig. 9 shows the average PAoI per link distance (rounded to 10 m) with different beacon rates that we obtained from the simulation. Indeed, we see that the link distance has an impact on the PAoI according to our hypothesis described previously.

For small link distances (less than 50 m) and low beacon rates (e.g., 1 Hz), the observed PAoI closely follows the beacon interval (i.e., the multiplicative inverse of the beacon rate) as the signal distortion due to the impact of the wireless communication channel is minimal. However, at higher beacon rates (e.g., 16 Hz), the effect is increased and becomes visible more clearly. Latest at roughly 400 m, we start to see a massive increase in PAoI, which is way above the beacon interval. Here, the probability for a successful reception of a packet is so low that many updates are lost and the PAoI increases a lot. For very high rates (e.g., 40 Hz and above), the PAoI already steeply rises at even low distances of below 100 m. As a result, we see that, even when using the same beacon rate, two links can have a very different PAoI because of different node distances. Hence, the freshness of the information from close vehicles is typically much better than from those far away, as expected.

5.4. Combined Standard AoI

Consider an arbitrary cooperative driving application that requires regular updates from surrounding vehicles (e.g., ICA, cf. Section 3). This application will likely define a target AoI (i.e., maximum allowed AoI) that is required by the application to work successfully and reliably. In order to determine whether certain information is fresh enough,

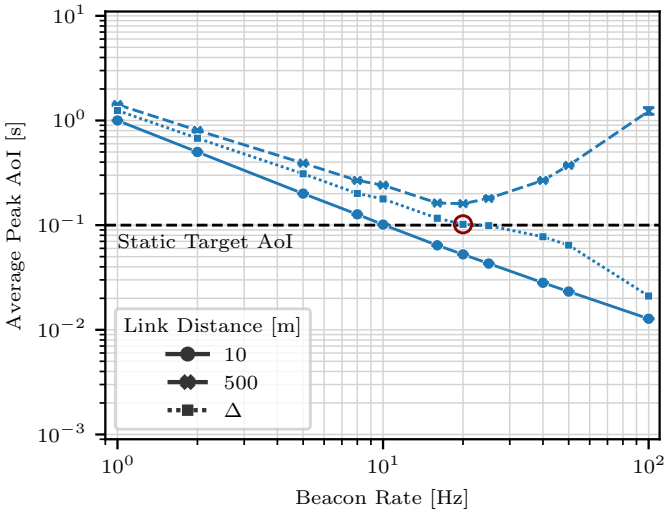

Figure 10: Average PAoI plotted for all as well as separated for two specific node distances (i.e., short and long). The red circle indicates the intersection of the average PAoI with the (static) target AoI of 100 ms.

the average PAoI can be evaluated against this requirement. A typical update interval requirement that is often found in literature is 100 ms [25, 26]. Following the observation from the previous section, far away vehicles will always suffer from a weakened SNIR and thus have a higher PAoI compared to vehicles that are close. Thus, when combining the PAoI values from all surrounding vehicles using Eq. (3), the far away vehicles will increase the average and thus distort the view on the overall information freshness.

Fig. 10 shows the average standard PAoI of short (i.e., 10 m) and long (i.e., 500 m) distance links for several beacon rates. It also shows a static target AoI of 100 ms as well as the average of the PAoI values from the two links (cf. Eq. (3)). As expected, the average PAoI of the short link distance (i.e., 10 m) continuously decreases proportional to the increasing beacon rate. Here, the minimum value, which indicates the best information freshness, is reached at the highest simulated beacon rate (i.e., 100 Hz. At this distance, the static target AoI of 100 ms is already reached at a beacon rate close to 10 Hz. This is expected, since 10 Hz is the multiplicative inverse of the target AoI and the PAoI is not distorted at these short distances (cf. Section 5.3).

When looking at the long link distance (i.e., 500 m), the situation is different: First, the average PAoI is decreasing similarly to the short link distance, following the increase of the beacon rate. But it never reaches the target AoI of 100 ms. Instead, after reaching its minimum at 20 Hz, the average PAoI increases when beacons are transmitted at higher rates. That is due to effects of the wireless communication channel described in Section 5.3.

When looking at the combination (i.e., average) of the two link distances, we can observe some interesting effects as well. First, the average PAoI value decreases as expected, but when increasing the beacon rate further, also its value decreases further, thus reaching the static target AoI of 100 ms at roughly 20 Hz (red circle). The continuous decrease even at higher beacon rates (i.e., above 20 Hz) is due to less received packets for the long distance link. Thus, the combined PAoI contains a lot more low values which have been observed from the short link distance.

When we now compare the beacon rates at which the static target AoI of 100 ms is met, we see that twice the beacon rate of the short distance links is required when combining the PAoI metrics from both distances. Hence, in order to keep the combined freshness of the information from all surrounding vehicles below the given AoI requirement, beacons need to be transmitted at a higher rate than required for close vehicles only. If vehicles now have different levels of relevance to the application, e.g., close vehicles are more important than far ones (cf. Section 3), the non-relevant vehicles (i.e., the far ones) will weaken the perceived combined information freshness. In order to meet the AoI requirement, all vehicles need to transmit their beacons at a higher rate, which leads to unnecessary transmissions and channel load.

5.5. Combined Weighted AoI

In order to cope with the issues of the standard AoI (i.e., effects of the wireless communication channel and equal importance of all nodes), we now apply the proposed spatial model from Section 3 to the AoI. Using Eq. (1), we calculate the weighting coefficient ω for every PAoI value that is observed for an arbitrary link between two vehicles i, j, producing a *weighted PAoI*. Additionally, we also apply the weighting coefficients to the static target AoI of 100 ms on a per link bases, producing a *weighted target AoI*. In this section, we use one exemplary parameterization (i.e., $\alpha = 0, \beta = 0.01$) of our spatial model that uses only the distance between vehicles for calculating the weighting coefficient. This focuses on the issue described in Section 5.3.

Fig. 11 shows the average weighted PAoI of short (i.e., 10 m) and long (i.e., 500 m) distance links over several beacon rates. It also shows an average weighted target AoI as well as the average PAoI values from the two links, which can be used by application as a view on the overall information freshness. Since we selected fixed distances, the calculated weighting coefficient will be the same for all links of the same distance. The resulting average weighted PAoI is just a multiplication of the average standard PAoI from Fig. 10 with a constant factor and thus follows a similar trend.

Due to the selected parameterization of our spatial model, a high (i.e., close to 1) and a low (i.e., close to 0) weighting coefficient is calculated for values of the short and long distance links, respectively. As a result, the average PAoI for the short distance links is very close to the one of the standard AoI from Fig. 10, whereas it is reduced a lot for the long distance links. Therefore, and due to less observations for the long distance links in general, the combination (i.e., average) of all PAoI values from both distances is, in comparison to Fig. 10, much closer to the

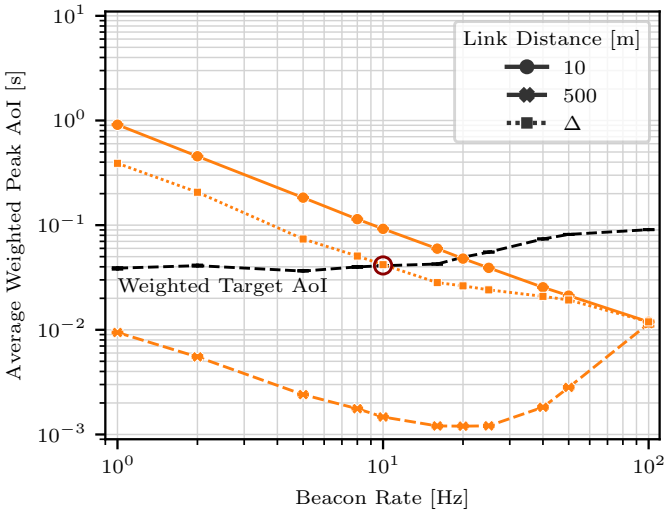

Figure 11: Average weighted PAoI for two specific link distances (i.e., short and long) and their combination (i.e., average). The red circle indicates the intersection of the combined PAoI with the weighted target AoI.

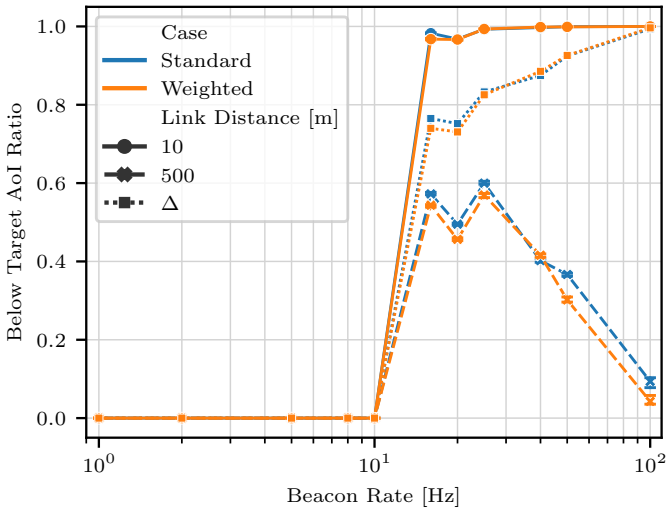

Figure 12: Ratio of vehicle updates that are below the target AoI for the standard case (blue) and when applying our spatial model (orange) – two specific link distances (i.e., short and long) and their combination (i.e., average).

average PAoI of the short distance links. Thus, the overall view on the information freshness is not distorted much by the long distance link, which is (in our parameterization) less relevant.

The average weighted target AoI is constructed by combining all weighted target AoI values from the two link distances, similarly to the average weighted PAoI. Since the same weighting coefficients are applied to the PAoI and the target AoI, the target faces similar effects: For the short distance, the target is close to the static target AoI of 100 ms, whereas for the long distance, it is close to 0 due to the weighting coefficient being close to 0. The average weighted target AoI thus is close to the static target AoI of 100 ms as it is mostly influenced by short distance links. Note that the individual weighted target AoI for both distances is constant for all beacon rates as the link distance does not change and the beacon rate is not considered when calculating the weighting coefficient. The average weighted target AoI, in contrast, is not constant due to the increasing number of lost packets and thus less values for the long link distance with high beacon rates. The average therefore tends towards the value of the short link distance, when using a beacon rate ≥ 20 Hz.

When comparing the average PAoI with the target AoI, we see that now both link distances as well as their combination intersect with the target AoI at some point. The short distance links meet the target at a beacon rate close to 20 Hz. The average PAoI of the long distance links is below the weighted target AoI even for all beacon rates. This is due to the average weighted target AoI mainly begin influenced by the short distance links, thus, tending towards the static target AoI of 100 ms. Additionally, the weighting coefficient for the long distance links are close to 0. The combined weighted PAoI reaches the weighted target AoI at a beacon rate close to 10 Hz, as indicated by the red circle. This is a smaller beacon rate than required for only the short distance links due to the impact of the long distance links on the average. However, we actually need to compare this situation with the values from using the standard PAoI and the static target AoI in Section 5.3: With the spatial model, we only need half of the previous beacon rate to reach the target AoI when combining all link distances. Using our model allows to focus on timely updates of relevant vehicles for meeting a given AoI requirement instead, which saves channel resources.

5.6. Ratio of Links Reaching the Target AoI

The weighted target which we introduced in Eq. (6) allows interpreting the weighted PAoI in the way we interpret the standard one. To illustrate the validity of our approach, Fig. 12 comparatively depicts the ratio of PAoI values fulfilling the condition in Eq. (7) and the case using the standard approach, i.e., $\Delta_{j,i} \leq T_{j,i}$ without using the weighting coefficient. Without the spatial model, the target AoI is static at 100 ms, whereas when applying the spatial model, it is calculated by using the weighting coefficient (cf. Eq. (6)).

The ratio for both cases is at 0 for all beacon rates ≤ 10 Hz. This is expected since the target AoI of 100 ms cannot be reached when the inter-arrival time of the beacons is larger than this value. When increasing the beacon rate further (above 10 Hz), all ratios are increasing as well. The ratios for the short link distance almost immediate reach 1 and stay there since these links have a very good SNIR and thus almost all transmitted beacons are received successfully, leading to a small PAoI. For the long link distance, the ratio grows as well but not as strongly as for the close links. Again, this is due to the weighted PAoI being impacted by the large distance of the link (cf. Fig. 9), thus leading to many PAoI values being above the target

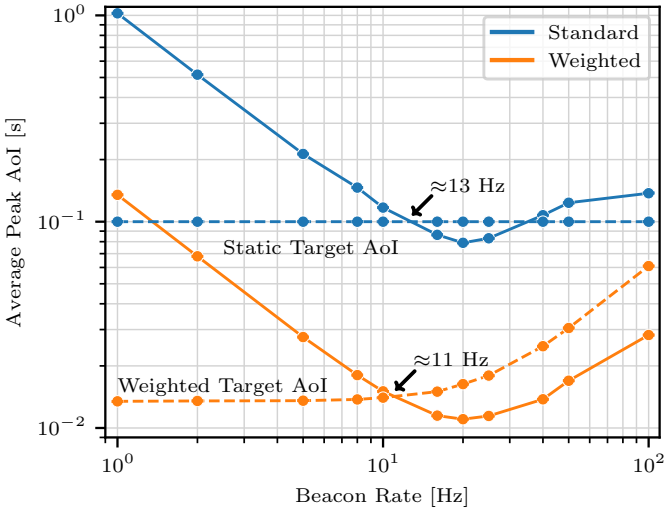

Figure 13: Average PAoI (solid) and corresponding target AoI (dashed) of the entire network for the standard case (blue) and when applying our spatial model (orange). The arrows indicate the intersection with the corresponding target AoI.

AoI. Beyond 25 Hz beacon rate, the ratio for the long link distance decreases again due to a high PAoI (cf. Fig. 11).

As expected, the combination of both link distances lies in between the short and the long distance links. After reaching roughly 0.75 at 16 Hz, its value increases until it reaches almost 1 at 100 Hz. This is due to the high number of lost packets for the long distance links, which leads to a value similar to the value of the short link distance.

It is visible that the ratio is very similar for both cases (i.e., standard and weighted). This reflects that the perceived status update on the network is the same irrespective of the weighting coefficients. Thus, using the formulation in Eq. (11) will not introduce any artifact on the perceived network status; instead, it will just emphasize the relevant links.

5.7. Weighted Network AoI

So far, in order to show how our spatial model can influence the perceived average PAoI when combining different links, we have been looking at two specific link distances only. Now, we combine all available links from within the simulation scenario to analyze the average PAoI of the entire network. Again, we are evaluating the freshness of the information by comparing the average PAoI against the AoI requirement. This time, however, the goal is to determine the overall information quality of the entire network.

Fig. 13 shows the average network PAoI (solid, cf. Eq. (4)) as well as the corresponding network target AoI (dashed) for the standard case (blue) and when applying our spatial model (orange). We use the same parameterization of the spatial model as we did already in Section 5.5 (i.e., $\alpha = 0, \beta = 0.01$). The standard PAoI (blue) behaves as expected. It follows the beacon rate inversely proportional as the interval between beacons decreases with higher beacon rates. It intersects with the static target AoI of 100 ms at approximately 13 Hz (not simulated) and reaches its minimum value at 20 Hz. Since the average PAoI here contains the values from all available link distances (i.e., 0–600 m), there is indeed a minimum, which we can not observe in Fig. 10. This is due enough successfully received packets with high PAoI values (mostly from long distance links) such that they can weaken the perceived average PAoI.

When looking at the weighted case (orange), the situation is similar but the absolute values of the average PAoI and target AoI are smaller due to the applied weighting coefficient. Note, that the minimum PAoI value is achieved at the same beacon rate in both cases, which underlines the applicability of our model without distorting the standard interpretation of the AoI. Similar to Fig. 11, the target is calculated by combining all available individual target AoI values using the average function (see Eq. (10)). It is almost constant and lower in comparison to the static target AoI at beacon rates ≤ 10 Hz due to many medium and long distance links that have a small weighting coefficient. At these low beacon rates, the packets from large distances can still be received successfully. When increasing the beacon rate beyond 10 Hz, analog to the average PAoI, the number of lost packets for medium and long distance links increases and the average weighted target AoI therefore tends towards the value of the short link distances. In the weighted case, the intersection of the average PAoI with the target happens already at approximately 11 Hz (not simulated), which indicates that this beacon rate is high enough to achieve the required AoI of the entire network on average. This approximated beacon rate is roughly 2 Hz lower compared to the standard case. Using our model thus allows to save channel resources by focusing on timely updates of relevant vehicles for meeting a given AoI requirement.

5.8. Impact of Model Parameters

In our simulative results, so far we have only looked at one exemplary parameterization (i.e., $\alpha = 0, \beta = 0.01$) of our spatial model that uses only the distance between vehicles for calculating the weighting coefficient. In fact, we used a very strict value for the distance parameter β, which was favouring very short link distances. In general, more relaxed configurations will lead to a higher weighting coefficient, thus, producing higher PAoI (cf. Section 5.1), especially for vehicles far away from the front of the receiver (i.e., in distance and orientation). Thus, we now compare the resulting average PAoI as well as the target AoI for different parameterizations of our spatial model.

Fig. 14 shows the average PAoI (solid) and corresponding target AoI (dashed) of the entire network for different configurations of our spatial model. Here, we focus only on 4 different configurations:

1. $\alpha = 0, \beta = 0$, which reflects the standard case by always using a weighting coefficient of 1 (blue),
2. $\alpha = 0, \beta = 0.01$, which only focuses on the distance

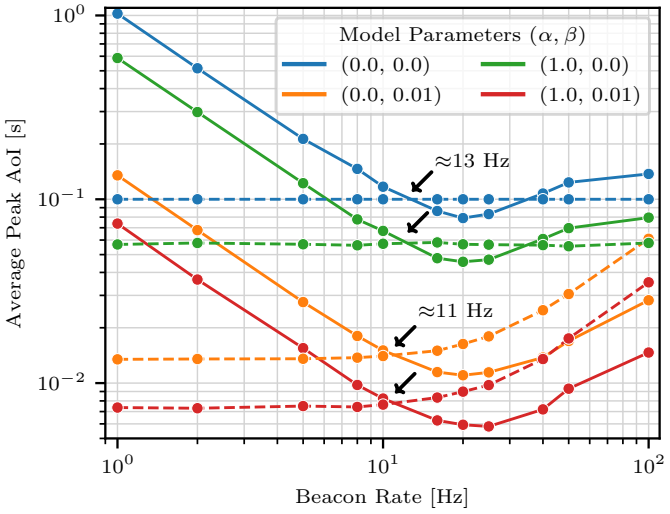

Figure 14: Average PAoI (solid) and corresponding target AoI (dashed) of the entire network for different configurations of our spatial model.

between vehicles for determining their relevance (orange, see previous sections),

3. $\alpha = 1, \beta = 0$, which only focuses on the orientation (angle) between vehicles for determining their relevance (green),

4. $\alpha = 1, \beta = 0.01$, which uses orientation (angle) and distance between vehicles for determining their relevance (red).

As expected, all configurations that apply our spatial model (i.e., 2–4) result in a decrease of the average PAoI and target AoI by filtering less relevant vehicles. We can observe, however, that using only the angle (2) results in a situation that is close to using the standard PAoI and the static target AoI (1). In contrast, using only the distance (3) results in a situation that is close to using angle and distance together (4). Configuration which behave similarly also have a similar beacon rate at which the average PAoI is intersecting with the target AoI, i.e., approximately 13 Hz vs. 11 Hz (not simulated). This shows that the distance has more impact than the angle when calculating the weighting coefficient, which is in line with the theoretical results from Section 5.1. This is due to the effects of the wireless communication channel (cf. Section 5.3), which impact the PAoI quite heavily. Also, vehicles within the scenario are distributed in space rather than in the close surroundings of single vehicles.

5.9. Impact of the Scenario

Until now, we had disabled all movement of the vehicles as well as the attenuation of the wireless signal by buildings in our Manhattan grid simulation scenario. We did this such that we can clearly observe the effects of our spatial model. It is obvious that this is not realistic and that enabling both of these will influence the wireless channel available to the vehicles.

When considering buildings, the wireless signal will be attenuated, leading to unsuccessful transmissions for links with medium and long distances, thus increasing their AoI (if a message is received at all). In contrast, the AoI for short link distances will likely be improved due to less interference from far-away vehicles. We expect this effect in particular within our Manhattan grid scenario as line-of-sight (LOS) between vehicles exists rarely, mainly only for vehicles on the same road or within the same road corridor. Additionally, every building's wall attenuates the signal of non line-of-sight (NLOS) links even more. Thus, the interference domain for every receiving vehicles is reduced a lot in comparison to the same scenario without buildings.

When considering mobility, the distance as well as the signal quality of the links will change over time as vehicles drive around. A former short distance link between two vehicles with a good signal quality can become a medium or even long distance one with worse quality (and AoI), and the other way around. However, in a free-space scenario, we expect these changes and the differences between vehicles to be limited and the link quality to stay rather equal as vehicles can only drive a certain distance in a given time and continuously have a LOS connection.

When considering the real-world scenario, i.e., combining attenuation by buildings and vehicle mobility, both of the aforementioned effects are mixed: At one point in time, an arbitrary link can have a good quality with a low AoI, but at a different point in time, the same link can have a very high AoI or be blocked completely because vehicles changed their position. The opposite can happen as well: vehicles that did not have a LOS connection before, leading to bad link quality and AoI values, can suddenly be on the same road corridor leading to a good LOS connection.

In order to show the impact of the three aforementioned cases in comparison to the previously used simulation scenario (i.e., free-space, no mobility), we repeated the previous simulation study with the following four scenarios:

1. *Freespace*, a scenario without buildings but with vehicle mobility

2. *Freespace static*, a scenario without buildings and without vehicle mobility (scenario from above)

3. *Manhattan*, a scenario with buildings and with vehicle mobility (real-word scenario)

4. *Manhattan static*, a scenario with buildings but without vehicle mobility

For these simulations, we set the simulation time to 30 s, such that the vehicle mobility can have an effect. In the remainder of this section, we only show results for the configurations $(0.0, 0.0)$ (standard case) and $(1.0, 0.01)$ (strictest weighted case, see Fig. 14).

In order to visualize the impact of the scenarios on networking metrics, Figures 15a and 15b shows simulation results for CBR and BRR, respectively. Values are recorded for all 200 vehicles during the entire simulation time and

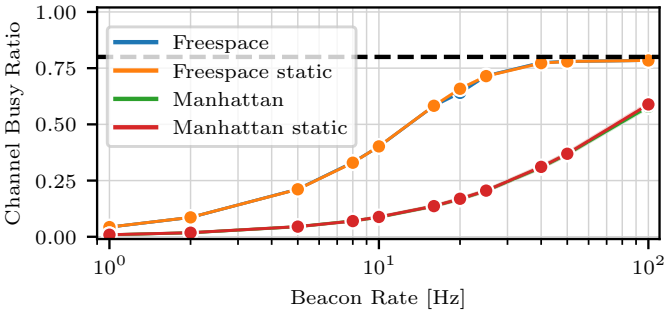

(a) Channel busy ratio (CBR). The dashed line indicates the practical maximum at 80% (cf. CSMA/CA in IEEE 802.11p).

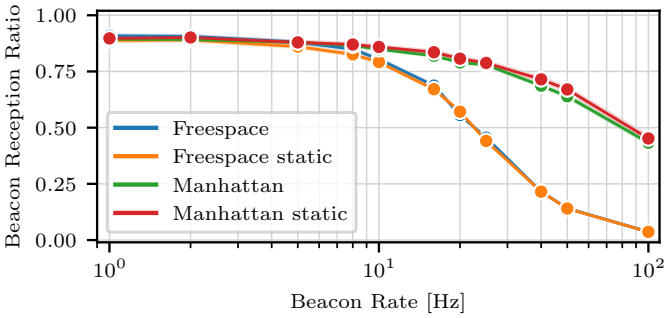

(b) Beacon reception ratio (BRR)

Figure 15: Key networking metrics for different scenarios.

are time-weighted averages, which we aggregate to overall averages. Since the spatial model does not impact these metrics, we do not visualize the different cases (standard vs. weighted). Following our expectations from above, buildings in the scenario have a huge impact on the signal quality and interference domain of vehicles and thus on the channel load. With buildings (*Manhattan* and *Manhattan static*), the wireless signals are heavily attenuated, leading to reduced absolute values and a less steep increase of the CBR in comparison to the scenarios without buildings. Even at high beacon rates (above 40 Hz), these scenarios still have a relatively low CBR whereas both scenarios without buildings reach the practical maximum value of 80% (cf. CSMA/CA in IEEE 802.11p). The results for the BRR are in line with the observed CBR: We observe a lot of collisions and thus lost beacons at high beacon rates, especially in the scenarios without buildings where the interference domain is large. In contrast to buildings, the vehicle mobility has only little impact on the channel load (see *static* vs. non-*static* scenarios) as the signal quality and interference domain does not change much by movement. This is inline with our expectations from above and can be observed in the BRR as well.

In order to analyze vehicles' knowledge of the scenario, we report the ratio of known neighbors (i.e., other vehicles from which at least 1 beacon was received) in Fig. 16. Again, we can observe the impact of the buildings, which block the signal of a lot of transmissions: While almost all other vehicles (neighbors) in the scenario are known (i.e., at least 1 beacon was received) within *Freespace* and

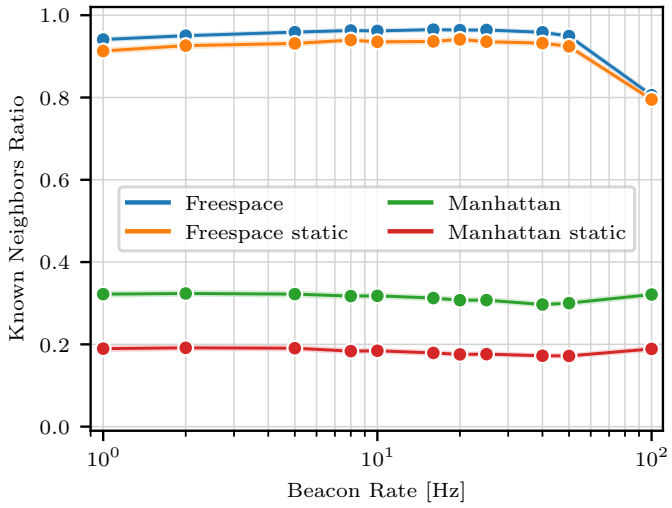

Figure 16: Average ratio of known neighbors (i.e., other vehicles from which at least 1 beacon was received) for different scenarios.

Freespace static, only some are known within *Manhattan* and *Manhattan static*. Here, the transmissions are blocked by the buildings, leading to no received beacons and thus no knowledge about a lot of other vehicles in the scenario. The values are (almost) constant over all (but the highest) beacon rates for all scenarios as the signal quality and interference domain does not change much due to vehicle movement and receiving at least 1 beacon during the entire simulation is possible even with high channel load (see Fig. 15a). This, of course, changes when requiring regular updates as packets are lost and updates are missed due to collisions. Following our expectations from above, mobility has only little impact for the scenarios without buildings. However, we can observe that it has indeed an impact and can increase the knowledge if the scenario contains buildings (*Manhattan* vs. *Manhattan static*). Here, mobility helps achieving links and thus knowledge about other vehicles by moving either into LOS or at least increasing signal quality for NLOS paths.

Fig. 17 shows the average network PAoI (solid and dotted lines) as well as the corresponding network target AoI (dashed lines) for all scenarios. Here, the solid lines correspond to the standard PAoI (no spatial model) whereas the dotted lines correspond to the weighted PAoI ($\alpha = 1.0, \beta = 0.01$). The latter one needs to be evaluated against the weighted the target AoI (colored dashed lines) whereas the standard case is evaluated against the target AoI of 100 ms (black dashed line).

Following the previously described effects, the spatial model reduces the values for PAoI and target AoI in all scenarios. The results for the scenarios without buildings (*Freespace static* and *Freespace*) are in line with Fig. 13 for both case: the PAoI follows the beacon rate, meets the target at 13 Hz and 11 Hz for the standard and weighted case, respectively, and increases again at higher beacon rates, which leads to a minimum at 20 Hz (for the standard case). Vehicle mobility here has almost no impact since all

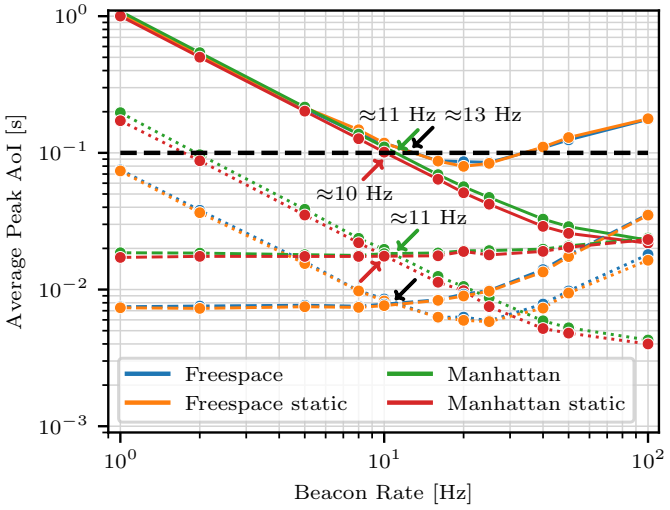

Figure 17: Average PAoI (solid and dotted lines) and corresponding target AoI (dashed lines) of the entire network for all scenarios). The solid lines show the standard PAoI wheres the dotted lines show the weighted PAoI with an exemplary configuration of $\alpha = 1.0, \beta = 0.01$. The corresponding target AoI is shown by the dashed lines (black = standard, color = weighted).

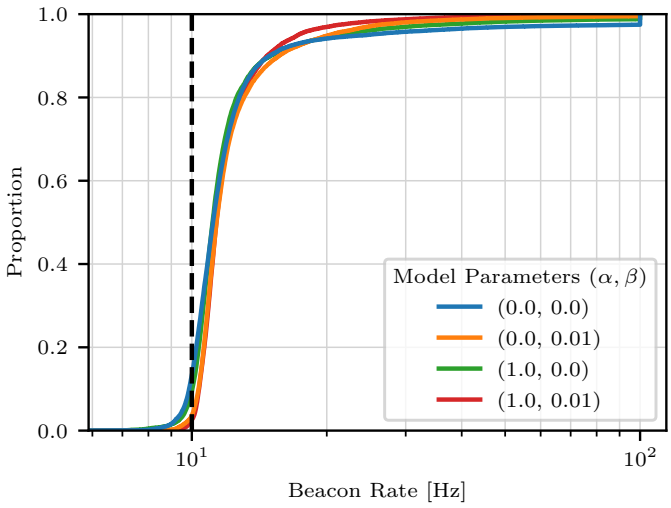

Figure 18: eCDF of observed beacon rate for the static target AoI of 100 ms for different configurations of our spatial model. The dashed line indicates the theoretical minimal required beacon rate in order to reach the target AoI (assuming no propagation delay and collisions).

vehicles already receive all signals and movement does not change the interference domain.

For scenarios with buildings (*Manhattan* and *Manhattan static*), we can observe some interesting effects. Both scenarios have smaller standard PAoI values because of the smaller interference domain and higher beacon reception ratio (see Fig. 15b) due to buildings. Accordingly, the channel will be saturated only at very high beacon rates, which leads to a minimal PAoI value at the highest simulated beacon rate of 100 Hz. Here, the PAoI behaves similarly to the short distance links from Section 5.4. Following the smaller beacon reception ratio from Fig. 15b, the vehicle mobility in the *Manhattan* scenario leads to slightly higher PAoI values. This is due to the fact that mobility achieves knowledge about *new* neighbors but increases the AoI for *old* neighbors at the same time.

When applying the spatial model, the PAoI as well as the target AoI is decreased as expected. However, they are still higher than the values of scenarios without buildings because the weighting coefficient $\omega_{i,j}$ overall has larger values. This is due to the current configuration of the spatial model ($\alpha = 1.0, \beta = 0.01$) and the overall smaller distances and limited set of angles for the links between vehicles due to the buildings (cf. Fig. 2). At the same time, the weighted target AoI is almost constant for both scenarios with buildings, being in-line with the metric of known neighbors (Fig. 16). The result of both of these effects is that the weighted PAoI reaches its corresponding target AoI at the same beacon rate ($\approx$ 10 Hz) as in the standard case. Thus, with this configuration of the spatial model, there is at least no visible benefit.

5.10. Adaptive Beaconing

In this section, we analyze the behavior of our AoI-based algorithm for adapting the beacon rate as well as the impact by the spatial model. We use the *Manhattan* scenario from Section 5.9 with buildings and vehicle mobility and a target AoI of 100 ms. Vehicles start with an initial beacon rate of 10 Hz, which is the theoretical minimal beacon rate required to reach the target AoI, assuming no propagation delay and packet collisions. We simulate for 30 s but treat the first 10 s as warm-up period, during which the beacon rate achieves a steady-state.

Fig. 18 shows the beacon rates observed from all vehicles in form of an empirical cumulative distribution function (eCDF) for different configurations of our spatial model. The adaptive algorithm leads to a beacon rate above the theoretical minimal beacon rate (10 Hz) required to reach the target AoI of 100 ms in most cases. In contrast, only a few values are below the minimum rate, leading to too infrequent updates in all configurations. However, the values are influenced by the configuration of our spatial model: In general, we can observe that applying our spatial model leads to a better beacon rate selection (a better fit to the required beacon rate of 10 Hz). This becomes more visible with stricter configurations (larger values of α and β, c.f Section 5.8). The beacon rates are less distributed (steeper eCDF curve) and closer to the theoretical minimal beacon rate. E.g., the mean value is at 12 Hz and 14 Hz for the strictest configuration (red) and the standard case (blue). In fact, the standard case has the most values below the minimal beacon rate of 10 Hz (13%) and above 20 Hz, which is double the minimal beacon rate, (6%). In comparison, the strictest weighted case has only 2% and 3% for low and high values, respectively. Similarly, the spatial model is able to reduce the amount of very large beacon rates: ≈24 Hz vs. ≈17 Hz for the 95th percentile,

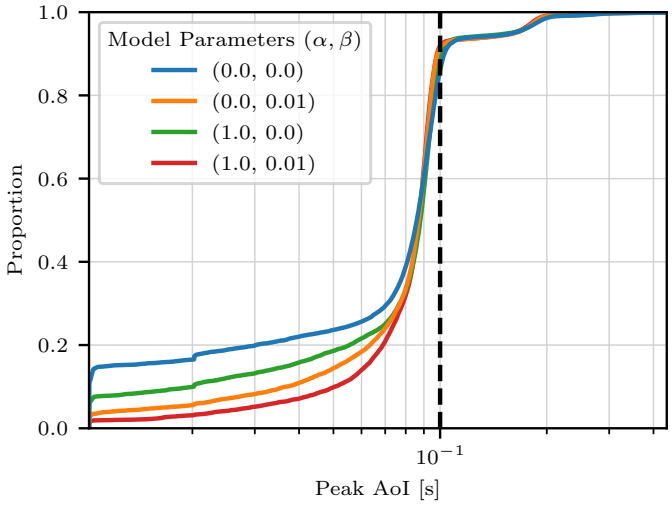

Figure 19: eCDF of observed PAoI for the target AoI of 100 ms (dashed line) for different configurations of our spatial model.

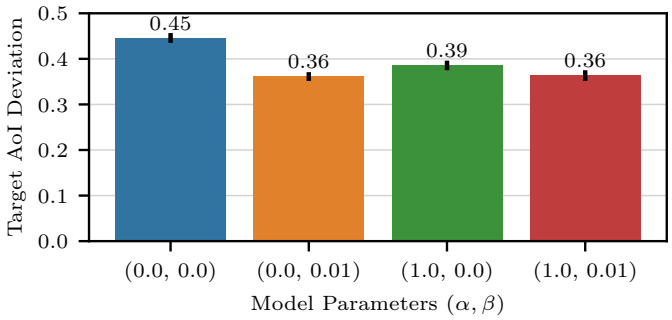

Figure 20: Average deviation (ratio) from target AoI of 100 ms for different configurations of our spatial model.

100 Hz (the maximum possible beacon rate) vs. ≈23 Hz for the 98th percentile, and 100 Hz vs. ≈33 Hz for the 99th percentile. The observed CBR follows accordingly with a mean of 12% vs. 10% and a 99th percentile of 18% vs. 16% for the standard case (blue) and the strictest model configuration (red). Overall, using the spatial model avoids outliers in both directions (too little and too high values) during beacon rate selection, which prevents too infrequent updates and high channel usage.

Fig. 19 shows the PAoI measurements observed from all vehicles in form of an eCDF for different configurations of our spatial model. Since the AoI is directly related to the beacon rate, the values follow the previously described effects (see Fig. 18): The stricter the spatial model configuration, the closer are the values to the target AoI of 100 ms, which serves as the set-point for the PID controller (see Section 4.2). Thus, the strictest configuration (red) has the largest but also closest PAoI values with the least spread. It has slightly higher mean PAoI values (0.08 s vs. 0.09 s) but leads to less deviation, e.g., 0.057 s vs. 0.074 s at the 25th percentile and 0.095 s vs. 0.092 s at the 75th percentile for the standard case (blue) and the strictest model configuration (red), respectively.

To visualize this effect more strongly, Fig. 20 shows the average deviation from target AoI of 100 ms for different configurations of our spatial model. Again, stricter model configurations lead to lower deviation, e.g., 67.5%, 45.7%, 38.4%, and 32.3% at the 75th percentile. In general, the overall performance of the system also increases when applying our spatial model: The strictest configuration reduces the outliers with large PAoI values from 0.21 s to 0.19 s at the 99th percentile. Thus, the ratio of observed PAoI measurements that are below their respective target AoI increases accordingly with stricter configurations (86%, 89.9%, 91.5%, and 92.3%). The remaining values above the target AoI correspond mostly to beacon rates smaller than 10 Hz (see Fig. 18).

6. Discussion & Remarks

Throughout this work, we used a static target AoI of 100 ms, since this value is often used in literature as a desired update interval for information used by cooperative driving applications. This value, however, is arbitrary and can freely be configured dependent on the specific needs of the chosen application. Our proposed spatial model is independent of the actual value for this target AoI, since the same weighting coefficient is applied to both, the observed PAoI values as well as the static target AoI. When modifying the value of the target AoI, the intersection point with the average PAoI will be shifted along the x-axes, leading to a different beacon rate that is sufficient for meeting the target. When the target value is increased, this beacon rate decreases and vice versa. In case both, a small target AoI and a low beacon rate, is desired, it can be beneficial to use a stricter configuration of our spatial model (i.e., lager values for α and β). This will impose a greater selectivity in the importance of vehicles and cope with effects of the wireless communication channel as described in Section 5.3.

We chose to aggregate PAoI values from multiple neighboring vehicles using the average function instead of some high percentile (e.g., 90th or 99th) due to multiple reasons. The average PAoI is a typical metric used in the field of age of information [3]. When using high percentiles instead of an average in order to focus on neighbors with bad freshness (i.e., high PAoI), the aggregated PAoI value will be worse (i.e., higher) and the target AoI will not be reached at all for the standard case. Applying our model in this case will result in an even better performance in comparison as the target AoI will still be reached (we do not show corresponding results within this manuscript).

The selection of the model parameters as well as the scenario play an important role in the resulting PAoI and target AoI values. A configuration which focuses mainly on the distance between vehicles is only useful if the interference domain is already large. In contrast, if the interference domain is small and observed AoI values of neighboring vehicles are similar, a different configuration is useful. The

mobility of vehicles did not play a big role within the results of our simulation study, but it can have a big impact on the knowledge of neighboring vehicles in scenarios with buildings.

Putting our spatial model to practical use within an AoI-based beacon adaption algorithm helps reaching an AoI requirement while avoiding strong outliers for the beacon rate. Accordingly, the channel usage is reduced and too infrequent updates are avoided. It should be noted that we used a very simple approach for controlling the beacon rate based on a PID controller. In fact, a PID controller is not well-suited for our use-case of keeping the PAoI below the target AoI as it tries to reach the set-point (the target AoI) exactly and treats positive & negative deviation from this value equally. A negative deviation from the set-point (i.e., PAoI lower than target AoI) is better (and even desired) than a positive deviation (which indicates outdated information). However, even with our simple approach, we are able to illustrate the benefit of applying the spatial model.

7. Conclusion

We explored the use of the age of information (AoI) in the context of intelligent transportation systems (ITS). First approaches of using the AoI in ITS focused on the original definition only, i.e., to measure the PAoIs for every received message and then to interpret the resulting values as they are. We, however, observed that this is not adequate in this application scenario as effects from the wireless communication channel may lead to quite variable PAoI measures for farther away vehicles – even though they play a less important role in many ITS applications.

In this paper, we proposed a new way of interpreting the AoI for arriving packets. We focus on the location of the transmitting vehicle as a metric to assess the importance of the information. Using a weighting coefficient applied to the PAoI and also to an AoI requirement, we can add a priority measure. As an example for ITS, we use the orientation and the distance of the corresponding vehicles for this process. It should be noted that the underlying PAoI metric is not changed in this procedure, i.e., compatibility with other approach is maintained. The benefit of applying the model is dependent on its parameters as well as the scenario, which requires careful configuration. Our spatial model allows to focus on timely updates of relevant vehicles for meeting a given AoI requirement, which helps saving resources on the wireless channel. Applying the model to an AoI-based beacon adaption algorithm thus increases information freshness while keeping beacon rates reasonable and resource usage small.

In future work, we plan to apply our spatial model to various different ITS applications to gain further insights to the advantages but also limits of the AoI metric in general. Based on the case-study in this work, more sophisticated protocols for adaptively adjusting the beacon rate based on the importance of the information to other vehicles can be build.

8. Acknowledgements

This work was supported in part by the Federal Ministry of Education and Research (BMBF, Germany) within the 6G Research and Innovation Cluster (6G-RIC) under grant 16KISK020K and the German Research Foundation (DFG) within the DyMoNet project under grant DR 639/25-1. The authors would like to thank M. Schettler for the support during the creation of this work.

References

[1] Falko Dressler, Florian Klingler, Michele Segata, and Renato Lo Cigno. Cooperative Driving and the Tactile Internet. *Proceedings of the IEEE*, 107(2):436–446, February 2019. ISSN 0018-9219. doi: 10.1109/JPROC.2018.2863026.

[2] ETSI. Intelligent Transport Systems (ITS); Vehicular Communications; Basic Set of Applications; Part 2: Specification of Cooperative Awareness Basic Service. EN 302 637-2 V1.3.2, European Telecommunications Standards Institute, November 2014.

[3] Roy D. Yates, Yin Sun, D. Richard Brown III, Sanjit K. Kaul, Eytan Modiano, and Sennur Ulukus. Age of Information: An Introduction and Survey. *IEEE Journal on Selected Areas in Communications (JSAC)*, 39(5):1183–1210, May 2021. ISSN 0733-8716. doi: 10.1109/jsac.2021.3065072.

[4] Antzela Kosta, Nikolaos Pappas, and Vangelis Angelakis. Age of Information: A New Concept, Metric, and Tool. *Foundations and Trends® in Networking*, 12(3):162–259, November 2017. ISSN 1554-0588. doi: 10.1561/1300000060.

[5] Wenrui Lin, Xijun Wang, Chao Xu, Xinghua Sun, and Xiang Chen. Average Age Of Changed Information In The Internet Of Things. In *IEEE Wireless Communications and Networking Conference (WCNC 2020)*, Virtual Conference, May 2020. IEEE. ISBN 978-1-7281-3106-1. doi: 10.1109/wcnc45663.2020.9120624.

[6] Sanjit K. Kaul, Marco Gruteser, Vinuth Rai, and John Kenney. Minimizing age of information in vehicular networks. In *8th Annual IEEE Communications Society Conference on Sensor, Mesh and Ad Hoc Communications and Networks (SECON 2011)*, Salt Lake City, UT, June 2011. IEEE. ISBN 978-1-4577-0093-4. doi: 10.1109/sahcn.2011.5984917.

[7] Federico Librino, M. Elena Renda, and Paolo Santi. Multihop Beaconing Forwarding Strategies in Congested IEEE 802.11p Vehicular Networks. *IEEE Transactions on Vehicular Technology (TVT)*, 65(9):7515–7528, September 2016. ISSN 1939-9359. doi: 10.1109/tvt.2015.2498284.

[8] Baiocchi Andrea and Ion Turcanu. A Model for the Optimization of Beacon Message Age-of-Information in a VANET. In *29th International Teletraffic Congress (ITC 2017)*, volume 1, pages 108–116, Genoa, Italy, September 2017. IEEE. doi: 10.23919/ITC.2017.8064345.

[9] Nikita Lyamin, Boris Bellalta, and Alexey Vinel. Age-of-Information-Aware Decentralized Congestion Control in VANETs. *IEEE Networking Letters*, 2(1):33–37, March 2020. ISSN 2576-3156. doi: 10.1109/lnet.2020.2970695.

[10] Baiocchi Andrea, Ion Turcanu, Nikita Lyamin, Katrin Sjöberg, and Alexey Vinel. Age of Information in IEEE 802.11p. In *17th IFIP/IEEE International Symposium on Integrated Network Management (IM 2021), 4th International Workshop on Intelligent Transportation and Autonomous Vehicles Technologies (ITAVT 2021)*, pages 1024–1031, Bordeaux, France, May 2021. IEEE. ISBN 978-3-903176-32-4.

[11] Baiocchi Andrea and Ion Turcanu. Age of Information of One-Hop Broadcast Communications in a CSMA Network. *IEEE*

Communications Letters, 25(1):294–298, January 2021. ISSN 1558-2558. doi: 10.1109/lcomm.2020.3022090.

[12] Liu Cao, Hao Yin, Ran Wei, and Lyutianyang Zhang. Optimize Semi-Persistent Scheduling in NR-V2X: An Age-of-Information Perspective. In *IEEE Wireless Communications and Networking Conference (WCNC 2022)*, pages 2053–2058, Austin, TX, April 2022. IEEE. ISBN 978-1-66544-267-1. doi: 10.1109/wcnc51071.2022.9771765.

[13] Roy D. Yates and Sanjit K. Kaul. The Age of Information: Real-Time Status Updating by Multiple Sources. *IEEE Transactions on Information Theory*, 65(3):1807–1827, March 2019. ISSN 0018-9448. doi: 10.1109/tit.2018.2871079.

[14] Clement Kam, Sastry Kompella, Gam D. Nguyen, Jeffrey E. Wieselthier, and Anthony Ephremides. Towards an effective age of information: Remote estimation of a Markov source. In *37th IEEE Conference on Computer Communications (INFOCOM 2018), 1st International Workshop on the Age of Information*, Honolulu, HI, April 2018. IEEE. doi: 10.1109/infcomw.2018.8406891.

[15] Jing Zhong, Roy D. Yates, and Emina Soljanin. Two Freshness Metrics for Local Cache Refresh. In *IEEE International Symposium on Information Theory (ISIT 2018)*, Vail, CO, June 2018. IEEE. doi: 10.1109/isit.2018.8437927.

[16] Ali Maatouk, Saad Kriouile, Mohamad Assaad, and Anthony Ephremides. The Age of Incorrect Information: A New Performance Metric for Status Updates. *IEEE/ACM Transactions on Networking (TON)*, 28(5):2215–2228, October 2020. ISSN 1063-6692. doi: 10.1109/tnet.2020.3005549.

[17] Julian Heinovski, Jorge Torres Gómez, and Falko Dressler. A Spatial Model for Using the Age of Information in Cooperative Driving Applications. In *25th ACM International Conference on Modeling, Analysis and Simulation of Wireless and Mobile Systems (MSWiM 2022)*, pages 85–94, Montréal, Canada, October 2022. ACM. ISBN 978-1-4503-9482-6. doi: 10.1145/3551659.3559053.

[18] David Jimenez-Soria, Beatriz Soret, and M. Carmen Aguayo-Torres. Experimental Characterization of Delay and Age of Information in DSRC V2V. In *96th IEEE Vehicular Technology Conference (VTC 2022-Fall)*, London, United Kingdom, September 2022. IEEE. ISBN 978-1-66545-468-1. doi: 10.1109/vtc2022-fall57202.2022.10012741.

[19] Alexey Vinel, Yevgeni Koucheryavy, Sergey Andreev, and Dirk Staehle. Estimation of a successful beacon reception probability in vehicular ad-hoc networks. In *5th International Conference on Wireless Communications and Mobile Computing Connecting the World Wirelessly (IWCMC 2009)*, Leipzig, Germany, June 2009. ACM Press. doi: 10.1145/1582379.1582470.

[20] Maria Michalopoulou, P. Kolios, C. Panayiotou, and G. Ellinas. A Framework for Minimizing Information Aging in the Exchange of CAV Messages. In *93rd IEEE Vehicular Technology Conference (VTC 2021-Spring)*, Virtual Conference, April 2021. IEEE. ISBN 978-1-7281-8964-2. doi: 10.1109/vtc2021-spring51267.2021.9448921.

[21] Jordi Marias I Parella, Olumide Ajayi, and Yu Cheng. Adaptive Messaging based on the Age of Information in VANETs. In *IEEE Global Telecommunications Conference (GLOBECOM 2022)*, pages 1235–1240, Rio de Janeiro, Brazil, December 2022. IEEE. ISBN 978-1-66543-540-6. doi: 10.1109/globecom48099.2022.10000671.

[22] Qiu Zhang, Nan Cheng, Ruijin Sun, and Dayue Zhang. AoI-Oriented Context-Aware Priority Design and Vehicle Scheduling Strategy in Vehicular Networks. In *IEEE/CIC International Conference on Communications in China (ICCC 2022), 2nd Workshop on Emerging Radio Access Network (eRAN) Technologies for B5G/6G*, pages 233–238, Sanshui, Foshan, China, August 2022. IEEE. ISBN 978-1-66545-978-5. doi: 10.1109/icccworkshops55477.2022.9896680.

[23] Ibrahim Sorkhoh, Dariush Ebrahimi, Sanaa Sharafeddine, and Chadi Assi. Minimizing the Age of Information in Intelligent Transportation Systems. In *9th IEEE International Conference on Cloud Networking (CloudNet 2020)*, Piscataway, NJ, November 2020. IEEE. ISBN 978-1-7281-9486-8. doi: 10.1109/cloudnet51028.2020.9335793.

[24] Lei Chen and Cristofer Englund. Cooperative Intersection Management: A Survey. *IEEE Transactions on Intelligent Transportation Systems (TITS)*, 17(2):570–586, February 2016. ISSN 1558-0016. doi: 10.1109/TITS.2015.2471812.

[25] Jeroen Ploeg, B.T.M. Scheepers, E. van Nunen, N. van de Wouw, and H. Nijmeijer. Design and Experimental Evaluation of Cooperative Adaptive Cruise Control. In *14th IEEE International Conference on Intelligent Transportation Systems (ITSC 2011)*, pages 260–265, Washington, D.C., October 2011. IEEE. doi: 10.1109/ITSC.2011.6082981.

[26] Julian Heinovski, Lukas Stratmann, Dominik S. Buse, Florian Klingler, Mario Franke, Marie-Christin H. Oczko, Christoph Sommer, Ingrid Scharlau, and Falko Dressler. Modeling Cycling Behavior to Improve Bicyclists' Safety at Intersections – A Networking Perspective. In *20th IEEE International Symposium on a World of Wireless, Mobile and Multimedia Networks (WoWMoM 2019)*, Washington, D.C., June 2019. IEEE. ISBN 978-1-7281-0270-2. doi: 10.1109/WoWMoM.2019.8793008.

[27] Jorge Torres Gómez, Ketki Pitke, Lukas Stratmann, and Falko Dressler. Age of Information in Molecular Communication Channels. *Elsevier Digital Signal Processing (DSP), Special Issue on Molecular Communication*, 124:103108, May 2022. ISSN 1051-2004. doi: 10.1016/j.dsp.2021.103108.

[28] A. Bruce Carlson, Paul B. Crilly, and Janet C. Rutledge. *Communication Systems: An Introduction to Signals and Noise in Electrical Communication*. McGraw-Hill, 4 edition, 2002. ISBN 978-0-07-011127-1.

[29] Yuanzhi Ni, Lin Cai, and Yuming Bo. Vehicular beacon broadcast scheduling based on age of information (AoI). *IEEE China Communications (CC)*, 15(7):67–76, July 2018. ISSN 1673-5447. doi: 10.1109/cc.2018.8424604.

[30] Nicolas Minorsky. Directional Stability of Automatically Steered Bodies. *Journal of the American Society for Naval Engineers*, 34 (2):280–309, March 1922. doi: 10.1111/j.1559-3584.1922.tb04958.x.

[31] Christoph Sommer, Reinhard German, and Falko Dressler. Bidirectionally Coupled Network and Road Traffic Simulation for Improved IVC Analysis. *IEEE Transactions on Mobile Computing (TMC)*, 10(1):3–15, January 2011. ISSN 1536-1233. doi: 10.1109/TMC.2010.133.

[32] Christoph Sommer, David Eckhoff, Reinhard German, and Falko Dressler. A Computationally Inexpensive Empirical Model of IEEE 802.11p Radio Shadowing in Urban Environments. In *8th IEEE/IFIP Conference on Wireless On demand Network Systems and Services (WONS 2011)*, pages 84–90, Bardonecchia, Italy, January 2011. IEEE. doi: 10.1109/WONS.2011.5720204.